Controlling the crystallization and magnetic properties of melt-spun Pr$_2$Fe$_{14}$B/α-Fe nanocomposites by Joule heating

Z. Q. Jin
School of Materials Science and Engineering, Georgia Institute of Technology, Atlanta, Georgia 30332
and Department of Physics, University of Texas at Arlington, Arlington, Texas 76019

B. Z. Cui
National High Magnetic Field Laboratory, Florida State University, Tallahassee, Florida 32310
and Department of Physics, University of Texas at Arlington, Arlington, Texas 76019

J. P. Liu[a),b)]
Department of Physics, University of Texas at Arlington, Arlington, Texas 76019

Y. Ding, Z. L. Wang, and N. N. Thadhani[a),c)]
School of Materials Science and Engineering, Georgia Institute of Technology, Atlanta, Georgia 30332

Pr$_2$Fe$_{14}$B/α-Fe based nanocomposites have been prepared through crystallization of melt-spun amorphous Pr$_7$Tb$_1$Fe$_{85}$Nb$_{0.5}$Zr$_{0.5}$B$_6$ ribbons by means of ac Joule heating while simultaneously monitoring room-temperature electrical resistance R. The R value shows a strong variation with respect to applied current I, and is closely related to the amorphous-to-nanocrystalline phase transformation. The curve of R versus I allows one to control the crystallization behavior during Joule heating and to identify the heat-treatment conditions for optimum magnetic properties. A coercivity of 550 kA/m and a maximum energy product of 128 kJ/m^3 have been obtained upon heating the amorphous ribbons at a current of 2.0 A. These properties are around 30% higher than the values of samples prepared by conventionally (furnace) annealed amorphous ribbons. © *2004 American Institute of Physics.* [DOI: 10.1063/1.1757017]

Exchange coupled R$_2$Fe$_{14}$B/(α-Fe or Fe$_3$B) (R = Pr,Nd) nanocomposites offer great promise as high performance magnets due to their high remanences.[1–7] It is noted that the magnetic behavior of these nanocomposites is closely related to grain size and nanostructured morphology. These nanocomposites can be prepared either by melt-spinning off-stoichiometric alloys at optimum speed or by subjecting amorphous alloys to a controlled crystallization annealing treatment.[2–4] However, the control of crystallization of amorphous precursors is critical for preparation of desirable nanostructures.[3,4] Samples crystallized from amorphous precursors usually present nonuniform and larger grain size morphology which significantly degrades the magnetic properties when compared with those samples crystallized from partially amorphous precursors. Therefore, grain growth inhibitors have been introduced to modify nucleation kinetics and prevent grain growth.[5–7] However, most nonmagnetic additives dilute magnetization. Another consideration is to increase heating rate in attempts to avoid the formation of undesired phases during the crystallization.[8] Recently, rapid thermal treatments via Joule heating have been successfully used to crystallize soft magnetic amorphous FeZrCuB alloys.[9,10] This technique allows crystallization to occur at higher temperatures in shorter duration than it does with conventional annealing,[11] and the crystallization behavior and nanostructure evolution can be easily followed through measurement of electrical resistance versus current curves. Here we report an approach to control the crystallization and magnetic properties of Pr$_2$Fe$_{14}$B/α-Fe based nanocomposite ribbons through monitoring electrical resistance during Joule heating.

Amorphous Pr$_7$Tb$_1$Fe$_{85}$Nb$_{0.5}$Zr$_{0.5}$B$_6$ ribbons were produced by melt-spinning of molten alloys at 35 m/s under an Ar atmosphere. The ribbons of ~1.1 mm width, ~30 μm thickness, and ~5 cm length were firmly clamped at opposite ends by a pair of electrical contacts and subjected to ac Joule heating in an Ar atmosphere. The applied voltage U was abruptly raised from zero to the desired value and retained for a desired duration up to 120 s, and then turned off to zero by abrupt interruption of power. The value of R at room temperature after Joule heating was considered for the description of applied current $I = U/R$. Selected amorphous ribbons were also annealed conventionally in a furnace under vacuum for 20 min at 650–800 °C to optimize magnetic properties. Crystallization of amorphous ribbons was determined from differential thermal analysis (DTA) traces measured by a Perkin-Elmer DTA7 at a heating rate of 20 K/min. The crystallized products were ascertained by performing x-ray diffraction analysis using Cu $K\alpha$ radiation. Magnetic properties were measured using a superconducting quantum interference device magnetometer with a maximum applied field of 70 kOe.

Figure 1(a) shows the heating time t dependencies of electrical resistance ratio R/R_0 and applied current I under constant voltage of 3.0 V. Here R_0 and R denote the room temperature electrical resistances of amorphous ribbon be-

---

[a)]Authors to whom correspondence should be addressed.
[b)]Electronic mail: pliu@uta.edu
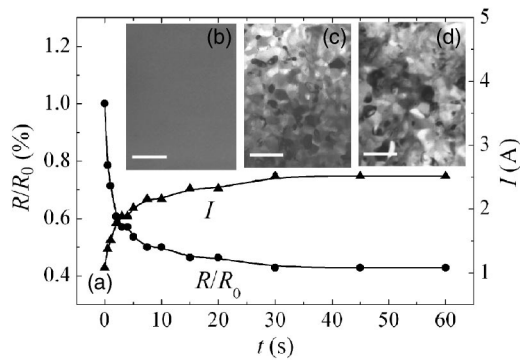[c)]Electronic mail: naresh.thadhani@mse.gatech.edu

FIG. 1. (a) Heating time t dependencies of electrical resistance ratio R/R_0 and applied current I at voltage of 3.0 V. Insets are TEM images of amorphous ribbon (b), and crystallized samples after Joule heating for (c) 2 s and (d) 5 s. (Bar length is 100 nm.)

FIG. 3. XRD patterns for samples prepared by Joule heating. The heating currents are indicated at the left. Inset is the grain size D of α-Fe as a function of current I.

fore and after Joule heating, respectively. A sharp drop in R/R_0 (up to 60%) is observed within initial 2 s due to massive crystallization of amorphous ribbons and the formation of nanocrystallites as evidenced in TEM images of Figs. 1(b)–1(d). The starting amorphous ribbon shows noncontrast characteristic while the samples prepared by Joule heating for 2 and 5 s show crystallite morphologies. It reveals that the short heating duration is sufficient to cause amorphous-to-crystalline phase transformation. Correspondingly, a rapid increase in the current also occurs within the same time scale. Prolonged heating time results in further decrease in R and increase in I, accompanied with the grain growth from 30 nm [Fig. 1(c)] to above 40 nm [Fig. 1(d)]. This shows that Joule heating is a nonisothermal process because the structural transformation upon heating alters the ribbon's electrical resistance and the current through the samples, which affect the heating temperature, and in turn, change the microstructure.[10,12]

Multistep heat treatments with successive increase of applied current for a duration of 5 s were used to analyze the crystallization process. Figure 2 shows a typical R/R_0-I curve measured during Joule heating of an amorphous ribbon. The current value I was taken as indicated in experiment methods. The value R/R_0 remains constant for I <0.7 A, indicating no significant structural transformation, after which a drastic decrease is observed. Since the variation in R/R_0 is sensitive to structure change and the fraction of amorphous/crystalline phase in the inhomogeneous system, any occurrence of new phases would be expected to result in
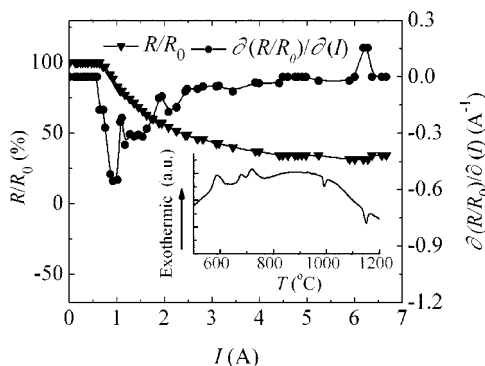
different amplitude of electrical resistance change. Thus the slight variation in drop rate in R/R_0-I curve can be displayed using its differential curve $\partial(R/R_0)/\partial(I)-I$ (denoted here as $J-H$ curve) to monitor the structural transformations. Three drops and one peak are observed in the $J-H$ curve. Similar $J-H$ curves were obtained for many amorphous samples, suggesting the crystallization process is reproducible. The peak at 6.3 A in the $J-H$ curve may be related to the structural change corresponding to the melting of $(Pr,Tb)_2(Fe,Nb,Zr)_{14}B$ (referred to as 2:14:1) phase. Finally the ribbon breaks above 6.7 A where iron melts. Of particular interest is the observation that $J-H$ curve has a similarity to DTA results (inset of Fig. 2) for amorphous sample. Three exothermic reactions are observed, the first one around 600 °C corresponding to the formation of α-Fe and $TbCu_7$ structure, and the other two to the formation of 2:14:1 and $Pr_{1+\delta}Fe_4B_4$ phases, respectively.[7] The two endothermic peaks at high temperatures are related to the melting points of 2:14:1 phase and iron, respectively.

The crystallization process associated with those drops on the $J-H$ curve for low currents has been determined by XRD patterns as shown in Fig. 3. The as-spun ribbons show an amorphous characteristic. Trace of crystallization of α-Fe appears at 0.7 A, immediately followed by nucleation of a metastable $TbCu_7$-type phase at 0.8 A, resulting in the first drastic drop in $J-H$ curve. A tiny amount of 2:14:1 precipitation phase occurs at 0.9 A. Upon heating above 1.1 A, a massive transformation from the $TbCu_7$-type phase to 2:14:1 phase can be observed, which leads to the second drop in $J-H$ curve. Some traces of Pr_2O_3 are observed for higher heating current. The XRD pattern gives no hint of texture formation. The average grain size of α-Fe, determined using Scherrer's formula, was found to increase from 10 to 27 nm with increasing current from 0.7 to 2 A as shown in the inset of Fig. 3. This is in good agreement with TEM observation. Upon heating above 2 A, no significant difference in phase structure was detected except for extensive grain growth to 38 nm for the sample heated at 5 A. The third drop in $J-H$ curve may be related to the precipitation of $Pr_{1+\delta}Fe_4B_4$ as minor phase as suggested by experiments on conventionally heated samples.[4] Thus, the results suggest that the characteristic $J-H$ curve can be used as a guide for studying the

FIG. 2. The curve of R/R_0 vs applied current I and the differential curve $\partial(R/R_0)/\partial(I)-I$. Inset is the result of DTA analysis on amorphous samples.
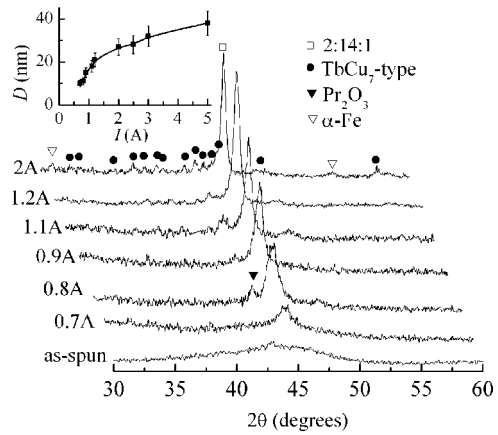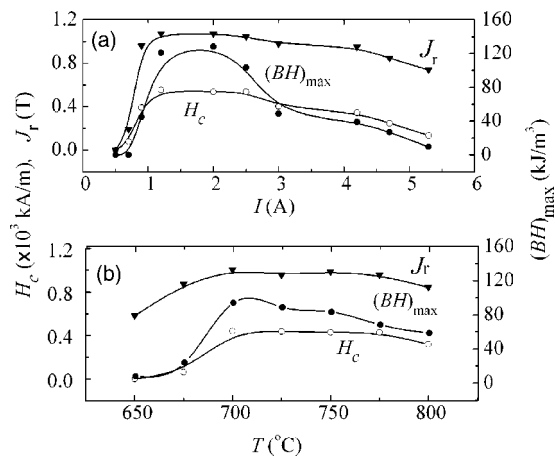
FIG. 4. Magnetic properties as functions of applied current I in case of Joule heating (a) and annealing temperature T in case of conventional (furnace) heating (b).

FIG. 5. Comparison of hysteresis loops of the samples prepared by conventional annealing at 700 °C for 20 min and by Joule heating at 2 A for 2 s.

crystallization behavior in attempts to optimize magnetic properties.

Figures 4(a) and 4(b) show the magnetic properties as functions of applied current I for Joule heating sample and annealing temperature T for conventionally (furnace) annealed samples, respectively. It can be seen that the samples heated below 0.7 A hardly show any coercivity H_c and remanence J_r. With increase of current, the improvement of magnetic properties was attributed to the formation of 2:14:1 phase. The current of 1.2–2 A results in high coercivities H_c of 540–550 kA/m. Optimal magnetic properties with remanence $J_r = 1.1$ T and maximum energy product $(BH)_{max} = 128$ kJ/m^3 were obtained in the samples heated at 2 A. For $I > 2.5$ A, the deterioration of magnetic properties may relate to the degradation of exchange interaction due to extensive grain coarsening as revealed in inset of Fig. 3. In case of conventionally (furnace) annealed samples, the optimal magnetic properties are $H_c = 440$ kA/m, $J_r = 1.0$ T, and $(BH)_{max} = 94$ kJ/m^3 for the sample annealed at 700 °C for 20 min. Higher annealing temperature and prolonged annealing time would result in deterioration of magnetic properties. It is noticed that these magnetic properties are lower than those optimal values of Joule heating samples. Figure 5 gives a comparison of hysteresis loops of samples prepared by these two different heating techniques. In the case of Joule heating samples, a better loop squareness originating from stronger exchange interaction between hard 2:14:1 and soft α-Fe phases leads to a $(BH)_{max}$ of around 30% larger than the value of conventionally (furnace) heated samples. The heating rate during Joule heating might be estimated to be greater than 350 K/s based on the assumption that the crystallization temperature of ~700 °C for 2:14:1 phase was achieved in heating duration of 2 s. The rapid heating rate leads to a
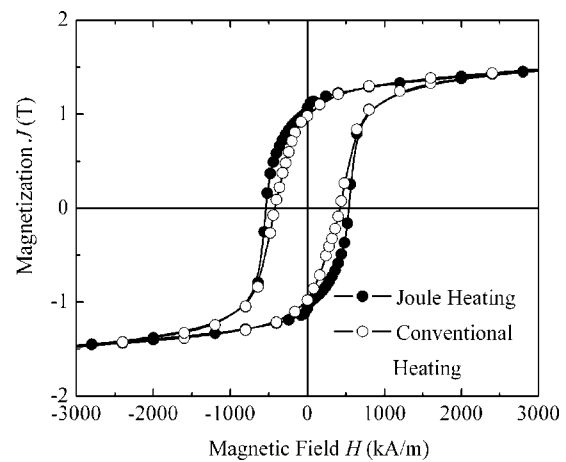
larger number density of nuclei, which may be helpful for obtaining a more fine nanostructure and responsible for the better magnetic properties. A small kink observed in the second quadrant suggests that the magnetic properties may be improved further by optimization of Joule heating conditions.

In conclusion, nonisothermal Joule-heating has been successfully applied to synthesize $Pr_2Fe_{14}B/\alpha$-Fe based nanocomposites with improved magnetic properties in comparison with conventional (furnace) heating. Of particular interest is the $R-I$ relationship, which has a good correlation with the crystallization behavior and provides an appropriate control of resulting phases in the nanocomposites. Therefore, optimal magnetic properties can be identified by monitoring the electrical resistance of the samples.

[1] E. F. Kneller and R. Hawig, IEEE Trans. Magn. **27**, 3588 (1991).
[2] J. Ding, P. G. McCormick, and R. Street, J. Magn. Magn. Mater. **124**, 1 (1993).
[3] Z. M. Chen, Y. Zhang, G. C. Hadjipanayis, Q. Chen, and B. M. Ma, J. Magn. Magn. Mater. **206**, 8 (1999).
[4] Z. Q. Jin, H. Okumura, J. S. Muñoz, Y. Zhang, H. L. Wang, and G. C. Hadjipanayis, J. Phys. D **35**, 2893 (2002).
[5] I. Betancourt and H. A. Davies, J. Magn. Magn. Mater. **261**, 328 (2003).
[6] K. Kajiwara, K. Hono, and S. Hirosawa, Mater. Trans., JIM **42**, 1858 (2001).
[7] Z. Q. Jin, H. Okumura, H. L. Wang, J. S. Muñoz, V. Papaefthymiou, and G. C. Hadjipanayis, J. Magn. Magn. Mater. **242**, 1307 (2002).
[8] A. Kojima, A. Makino, and A. Inoue, J. Appl. Phys. **87**, 6576 (2000).
[9] E. Estevez-Rams, J. Fidler, M. Dahlgren, R. Grössinger, M. Knobel, P. Tiberto, P. Allia, and F. Vinai, J. Phys. D **29**, 848 (1996).
[10] F. C. S. da Silva, E. F. Ferrari, M. Knobel, I. L. Torriani, and D. R. dos Santos, Appl. Phys. Lett. **77**, 1375 (2000).
[11] P. Gorria, I. Orue, F. Plazaola, and J. M. Barandiaran, J. Appl. Phys. **73**, 6600 (1993).
[12] P. Allia, M. Baricco, P. Tiberto, and F. Vinai, Phys. Rev. B **47**, 3118 (1993).